

Performance Analysis of Quantum Error-Correcting Codes via MacWilliams Identities

Diego Forlivesi, *Student Member, IEEE*,

Lorenzo Valentini, *Student Member, IEEE*, and Marco Chiani, *Fellow, IEEE*

Abstract

One of the main challenges for an efficient implementation of quantum information technologies is how to counteract quantum noise. Quantum error correcting codes are therefore of primary interest for the evolution towards quantum computing and quantum Internet. We analyze the performance of stabilizer codes, one of the most important classes for practical implementations, on both symmetric and asymmetric quantum channels. To this aim, we first derive the weight enumerator (WE) for the undetectable errors of stabilizer codes based on the quantum MacWilliams identities. The WE is then used to evaluate the error rate of quantum codes under maximum likelihood decoding or, in the case of surface codes, under minimum weight perfect matching (MWPM) decoding. Our findings lead to analytical formulas for the performance of generic stabilizer codes, including the Shor code, the Steane code, as well as surface codes. For example, on a depolarizing channel with physical error rate $\rho \rightarrow 0$ it is found that the logical error rate ρ_L is asymptotically $\rho_L \rightarrow 16.2\rho^2$ for the $[[9, 1, 3]]$ Shor code, $\rho_L \rightarrow 16.38\rho^2$ for the $[[7, 1, 3]]$ Steane code, $\rho_L \rightarrow 18.74\rho^2$ for the $[[13, 1, 3]]$ surface code, and $\rho_L \rightarrow 149.24\rho^3$ for the $[[41, 1, 5]]$ surface code.

I. INTRODUCTION

The exploitation of the unique features of quantum mechanics has opened new perspectives on how we can sense, process, and communicate information [1]–[6]. From an engineering point of view, there are many challenges to solve, calling for both theoretical and experimental research studies. The aim is to progress towards the already known possible applications of

The authors are with the Department of Electrical, Electronic, and Information Engineering “Guglielmo Marconi” and CNIT/WiLab, University of Bologna, 40136 Bologna, Italy. E-mail: {diego.forlivesi2,lorenzo.valentini13,marco.chiani}@unibo.it. Part of this work will be presented at IEEE ICC 2023, Rome, May 2023 (*arXiv:2302.13015*).

quantum information technologies, as well as those currently still unforeseen, that will arise when practical implementations become available. One of the main challenges is how to deal with the noise caused by unwanted interaction of the quantum information with the environment [7]–[13]. Quantum error correcting codes, where a redundant representation of quantum states protects from certain types of errors, are therefore of paramount importance for quantum computation, quantum memories, and quantum communication systems [7]–[21].

Quantum error correction is made difficult by the laws of quantum mechanics which imply that qubits cannot be copied or measured without perturbing state superposition. Moreover, there is a continuum of errors that could occur on a qubit. However, it has been shown that in order to correct an arbitrary qubit error it is sufficient to consider error correction on the discrete set of Pauli operators [10], [12], [15]. Thus, we can consider in general a channel introducing qubit Pauli errors \mathbf{X} , \mathbf{Y} , and \mathbf{Z} with probabilities p_X , p_Y , and p_Z , respectively, and leaving the qubit intact with probability $1 - \rho$, where $\rho = p_X + p_Y + p_Z$. A special case of this model is the so-called depolarizing (or symmetric) channel for which $p_X = p_Y = p_Z = \rho/3$. Quantum error-correcting codes for this channel are thus designed to protect against equiprobable Pauli errors [7], [8], [12], [14], [22]. However, depending on the technology adopted for the system implementation, the different types of Pauli error can have different probabilities of occurrence, leading to polarizing (or asymmetric) quantum channels [23]–[26].

In this paper we provide an analytical evaluation of the performance of generic stabilizer codes, including surface codes [9], [12], [27]–[31]. Stabilizer codes are indeed the most important class of quantum error correcting codes (QECCs) for practical implementations. However, despite their importance, the performance of these codes has been investigated in the literature only partially, and mainly in terms of accuracy threshold over symmetric channels for fault-tolerant quantum computing [9], [12], [27], [28], [32]–[34]. Here we propose a framework for the performance investigation of stabilizer codes by means of the quantum MacWilliams identities, leading to analytical expressions for the logical error rates, assuming maximum likelihood (ML) decoding or, for the surface codes, MWPM decoding. The analysis is carried out for both symmetric and asymmetric models for the quantum channel errors.

The key contributions of the paper can be summarized as follows:

- we derive the WE for the undetectable errors of arbitrary stabilizer codes via MacWilliams identities;
- we derive analytical expressions for the performance of stabilizer codes under ML

decoding, over symmetric and asymmetric channels;

- we derive analytical expressions for the performance of surface codes under MWPM decoding, over symmetric and asymmetric channels;
- we study the asymptotic behavior of the error probability, and introduce the concept of code-effective threshold.

As relevant examples, we give the expressions for the performance of the Shor code, the Steane code, and of surface codes. When analyzing surface codes, we will focus in particular on the $[[13, 1, 3]]$, the $[[23, 1, 3/5]]$, the $[[33, 1, 3/7]]$, and the $[[41, 1, 5]]$ codes.

This paper is organized as follows. Section II introduces preliminary concepts and models together with some background material. Sections III and IV provide the analytical investigation of QECC with bounded distance, and with complete decoding. In Section V we derive the WE for the undetectable errors from MacWilliams identities and apply it to the evaluation of the logical error rate of arbitrary stabilizer codes. Numerical results are discussed in Section VI.

II. PRELIMINARIES AND BACKGROUND

A. Quantum Error Correction

A qubit is an element of the two-dimensional Hilbert space \mathcal{H}^2 , with basis $|0\rangle$ and $|1\rangle$ [12]. The Pauli operators \mathbf{I} , \mathbf{X} , \mathbf{Z} , and \mathbf{Y} , are defined by $\mathbf{I}|a\rangle = |a\rangle$, $\mathbf{X}|a\rangle = |a \oplus 1\rangle$, $\mathbf{Z}|a\rangle = (-1)^a|a\rangle$, and $\mathbf{Y}|a\rangle = i(-1)^a|a \oplus 1\rangle$ for $a \in \{0, 1\}$. These operators either commute or anticommute with each other. We indicate with $[[n, k, d]]$ a QECC with minimum distance d , that encodes k information qubits $|\varphi\rangle$ (called logical qubits) into a codeword of n qubits $|\psi\rangle$ (called data or physical qubits), allowing the decoder to correct all patterns up to $t = \lfloor (d-1)/2 \rfloor$ errors (and some patterns of more errors). The codewords will be assumed equiprobable in the following. Using the stabilizer formalism, we start by choosing $n-k$ independent and commuting operators $\mathbf{G}_i \in \mathcal{G}_n$, called stabilizer generators (or simply generators), where \mathcal{G}_n is the Pauli group on n qubits [12], [15]. The subgroup of \mathcal{G}_n generated by all combinations of the $\mathbf{G}_i \in \mathcal{G}_n$ is a stabilizer, indicated as \mathcal{S} . The code \mathcal{C} is the set of quantum states $|\psi\rangle$ stabilized by \mathcal{S} , i.e., satisfying $\mathbf{S}|\psi\rangle = |\psi\rangle \forall \mathbf{S} \in \mathcal{S}$, or, equivalently, $\mathbf{G}_i|\psi\rangle = |\psi\rangle, i = 1, 2, \dots, n-k$. For a subgroup \mathcal{H} of a group \mathcal{G} we indicate with $\mathcal{N}(\mathcal{H})$ the normalizer, and with $\mathcal{C}(\mathcal{H})$ the centralizer. The centralizer and the normalizer of the stabilizer \mathcal{S} are coincident, $\mathcal{N}(\mathcal{S}) = \mathcal{C}(\mathcal{S})$.

Assume a codeword $|\psi\rangle \in \mathcal{C}$ is affected by a channel error. Measuring the received state according to the generators \mathbf{G}_i with the aid of ancilla qubits, the error collapses on a discrete set of possibilities represented by combinations of Pauli operators $\mathbf{E} \in \mathcal{G}_n$ [15]. Thus, an error can be described by specifying the single Pauli errors on each qubit. The measurement procedure over the ancilla qubits results in a quantum error syndrome $\mathbf{s}(\mathbf{E}) = (s_1, s_2, \dots, s_{n-k})$, with each $s_i = 0$ or 1 depending on \mathbf{E} commuting or anticommuting with \mathbf{G}_i , respectively [15]. Note that an error $\mathbf{E} \in \mathcal{S}$ has no effect on a codeword since in this case $\mathbf{E}|\psi\rangle = |\psi\rangle$.

A maximum likelihood decoder will infer the most probable error $\hat{\mathbf{E}} \in \mathcal{G}_n$ compatible with the measured syndrome. The weight of an error is the number of single Pauli errors (\mathbf{X} , \mathbf{Z} , and \mathbf{Y}) that occurred on a codeword. For example, the error $\mathbf{E} = \mathbf{X}_2\mathbf{Y}_3$ has weight two, with \mathbf{X} occurred on the second qubit, and \mathbf{Y} occurred on the third qubit.

A simple channel model is one characterized by errors occurring independently and with the same statistic on the individual qubits of each codeword. In this model, the error on each physical qubit can be \mathbf{X} , \mathbf{Z} or \mathbf{Y} with probabilities p_X , p_Z , and p_Y , respectively. The probability of a generic error on a physical qubit is $\rho = p_X + p_Z + p_Y$. Two important models are the *depolarizing channel* where $p_X = p_Z = p_Y = \rho/3$, and the *phase flip channel* where $\rho = p_Z$, $p_X = p_Y = 0$. We will also consider more general asymmetric channels with the constraint $p_X = p_Y$, therefore completely characterized by the bias parameter $A = 2p_Z/(\rho - p_Z)$. Note that for $A = 1$ we have the depolarizing channel, and for $A \rightarrow \infty$ we have the phase flip channel.

In the following, we will also adopt the notation $[[n, k, d_X/d_Z]]$ for asymmetric codes able to correct all patterns up to $t_X = \lfloor (d_X - 1)/2 \rfloor$ Pauli \mathbf{X} errors and $t_Z = \lfloor (d_Z - 1)/2 \rfloor$ Pauli \mathbf{Z} errors.

B. Quantum Topological Codes

One of the most important families of stabilizer QECC is that of *topological* codes. The general design principle behind these codes is that they are built by patching together repeated elements. Using this kind of approach, they can be easily scaled in size in order to increase the distance of the code, still guaranteeing commutativity of the generators. As regards the actual implementation, these codes have a great intrinsic advantage. In fact, they require only nearest-neighbor interactions. This is an important property since it seems difficult, for current quantum implementations of encoders and decoders, to perform high-fidelity long-range operations between qubits [18].

The most important codes within this category are the *surface* codes, in which all the check operators are local and the qubits are arranged on planar sheets. Each stabilizer is associated either with one of the sites or one of the cells that are called “plaquettes”. In this structure, logical qubits are defined using spare degrees of freedom in the lattice [35]. A common way of doing so consists in defining a lattice having boundaries with two different kinds of edges. In this case, the stabilizer’s generators in the interior are four-qubits plaquette or site operators, while the ones at the boundaries are three-qubits operators. Along a plaquette or “rough” edge, each generator is a three-qubits operator $Z^{\otimes 3}$, while, along a site edge or “smooth” edge, each generator is a three-qubits operator $X^{\otimes 3}$. Using this procedure, only a single degree of freedom is introduced, hence the entire lattice is able to encode just one logical qubit ($k = 1$). Thus, an information qubit $|\varphi\rangle = \alpha|0\rangle + \beta|1\rangle$ is encoded into $|\psi\rangle = \alpha|0_L\rangle + \beta|1_L\rangle$, where $|0_L\rangle$ and $|1_L\rangle$ are composed by n qubits. It can be shown that in a code with distance d , the lattice has $d^2 + (d - 1)^2$ links, which correspond to physical qubits [36]. For example, two equivalent graphical representations of the resulting lattice for the $[[13, 1, 3]]$ surface code are shown in Fig. 1. For this surface code, the generators are

$$\begin{aligned} G_1 &= X_1 X_2 X_4 & G_2 &= X_2 X_3 X_5 \\ G_3 &= Z_1 Z_4 Z_6 & G_4 &= Z_2 Z_4 Z_5 Z_7 & G_5 &= Z_3 Z_5 Z_8 \\ G_6 &= X_4 X_6 X_7 X_9 & G_7 &= X_5 X_7 X_8 X_{10} \\ G_8 &= Z_6 Z_9 Z_{11} & G_9 &= Z_7 Z_9 Z_{10} Z_{12} & G_{10} &= Z_8 Z_{10} Z_{13} \\ G_{11} &= X_9 X_{11} X_{12} & G_{12} &= X_{10} X_{12} X_{13}. \end{aligned}$$

Note that applying a Pauli operator that commutes with all the generators will preserve the code space. The definition of the logical X_L and Z_L operators for the code is straightforward. In particular, the logical Z_L operator can be chosen as a tensor product of Z ’s acting on a chain of qubits running from a rough edge to the one at the opposite side of the lattice. Similarly, the X_L logical operator will be the tensor product of X ’s acting on a chain running from a smooth link to the correspondent one at the other side of the dual lattice. As an example, the 13 qubits surface code, with distance 3, is shown in Fig. 1.

In addition to the previous properties, surface codes have a great advantage: the value of their accuracy threshold is 0.11 [36]. This is important because, according to the threshold theorem, the logical error rate can be lowered at will, by increasing the code size, if the qubits physical error rate is below this threshold [18]. Another important feature is that a simple complete decoder exists for such codes: the MWPM [37]. This decoder finds the shortest

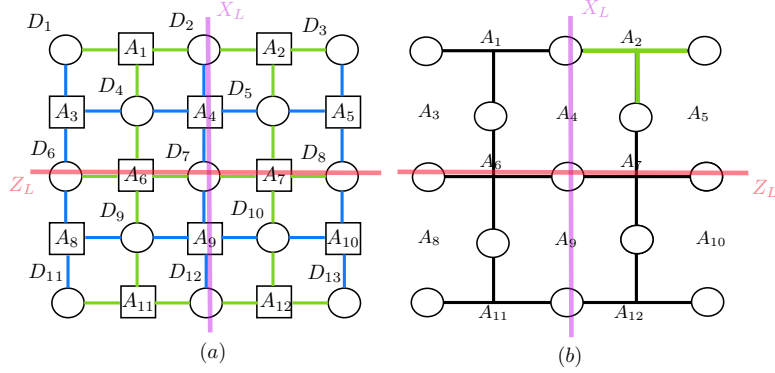


Fig. 1. $[[13, 1, 3]]$ Surface code. (a) Actual lattice with data qubits (circles) and ancillae (squares). (b) Simplified representation with X generators corresponding to sites and Z generators to plaquettes. A smooth edge and a rough edge are depicted in green and blue, respectively. Examples of logical operators are drawn on the lattice.

way to connect pairs of changed ancillae. Moreover, the structure of their lattice provides an intrinsic advantage during the decoding. Indeed, it was explained above that any set of Z (X) operators which form a closed loop on the edges of the lattice (including the link which is missing in each boundary plaquette) is contained in the stabilizer. Hence, if the decoder chooses a wrong error chain, but the correction operator together with the channel error closes a loop, the error is correctly recovered. As a consequence, surface codes can also easily correct a large number of errors with a weight larger than $t = \lfloor (d-1)/2 \rfloor$. For instance, it will be shown that the MWPM decoder for the $[[13, 1, 3]]$ surface code is able to correct, besides all errors of weight one, many errors with weight $w = 2$ and a good amount of errors with weight $w = 3, 4, 5$ and 6 . In general, a decoding error occurs every time that the concatenation of actual channel error and correction operator realizes a logical operator, so the whole chain operator crosses the lattice from boundary to boundary. For instance, consider a two qubits error Z_2Z_3 for the code in Fig. 1. In this scenario, the ancilla qubit A_1 is the only one that changes its state, hence the decoder assumes (wrongly) an error Z on data qubit D_1 . It can be easily noticed that the whole operator applied to the lattice represents the logical Z_L .

Rectangular surface codes, having horizontal and vertical dimensions of different lengths, can be used over asymmetric channels. For example, since Z errors often happen more frequently in hardware implementations [23], [26], [38], we could consider the $[[23, 1, 3/5]]$ surface code, in which the horizontal direction is two-qubit longer than the vertical one, making the logical Z_L operator a chain of 5 qubits (not 3 like in the $[[13, 1, 3]]$ code). A code of this kind requires a lattice of 23 qubits but it has a distance $d_Z = 5$, so it is able to

correct Z errors of weight $w = 2$.

III. QUANTUM CODES WITH BOUNDED DISTANCE DECODING

The codeword error probability, ρ_L , also called logical error probability, is defined as the probability that the decoder does not correct the errors introduced by the quantum channel.

A. Symmetric Codes

Let us first assume an $[[n, k, d]]$ QECC together with a decoder which corrects up to $t = \lfloor (d-1)/2 \rfloor$ generic errors (i.e., X , Z , or Y) per codeword, and no others. For this bounded distance (BD) decoder, the logical error probability is simply

$$\rho_L = 1 - \sum_{j=0}^t \binom{n}{j} \rho^j (1-\rho)^{n-j} \quad (1)$$

that, for $\rho \ll 1$, can be approximated as

$$\rho_L \simeq \binom{n}{t+1} \rho^{t+1}. \quad (2)$$

We can see that the slope in the log-log plot of the logical error probability ρ_L vs. the physical error probability ρ is $t+1$.

B. Asymmetric Codes

The error probability analysis has been recently generalized to asymmetric QECCs assuming a decoder able to correct up to e_g generic errors plus up to e_Z Pauli Z errors per codeword, and no others. In this case, weighting each pattern with the corresponding probability of occurrence, the bounded distance decoding error rate (1) over an asymmetric quantum channel with arbitrary p_X , p_Y , and p_Z becomes [26]

$$\rho_L = 1 - \sum_{j=0}^{e_g+e_Z} \binom{n}{j} (1-\rho)^{n-j} \sum_{i=(j-e_g)^+}^j \binom{j}{i} p_Z^i (\rho - p_Z)^{j-i} \quad (3)$$

where $(x)^+ = \max\{x, 0\}$. For a channel with asymmetry parameter $A = 2p_Z/(\rho - p_Z)$, the expression in (3) can be rewritten

$$\rho_L = 1 - \sum_{j=0}^{e_g+e_Z} \alpha_j \binom{n}{j} \rho^j (1-\rho)^{n-j} \quad (4)$$

where

$$\alpha_j = \begin{cases} 1 & \text{if } j \leq e_g \\ \left(\frac{2}{A+2}\right)^j \sum_{i=j-e_g}^j \binom{j}{i} \left(\frac{A}{2}\right)^i & \text{otherwise.} \end{cases} \quad (5)$$

Note that, when the code is symmetric $e_Z = 0$, and (4) reduces to (1).

Starting from (4), the asymptotic slope analysis can be extended to asymmetric codes with $e_Z \geq 1$, giving for $\rho \ll 1$

$$\rho_L \simeq \begin{cases} \binom{n}{e_g+1} \left(\frac{2\rho}{A+2}\right)^{e_g+1} & 1 \leq A < \infty \\ \binom{n}{e_g+e_Z+1} \rho^{e_g+e_Z+1} & A \rightarrow \infty. \end{cases} \quad (6)$$

We observe that in this case, the asymptotic slope is $e_g + 1$ for all finite A . On the other hand, considering a phase flip channel ($A \rightarrow \infty$) the slope becomes $e_g + e_Z + 1$.

IV. QUANTUM CODES WITH COMPLETE DECODING

Let us now assume to have a decoder that always tries to correct the errors (complete decoder). This could allow correcting also some (but not all) error patterns which are not correctable with bounded distance decoding. Two examples are the ML decoder (complex for large codes), and the MWPM decoder (for surface codes).

Definition 1. We indicate with β_j the fraction of errors of weight j that can be corrected by a complete decoder.

Note that β_j depends in general on the code structure, on the decoder, and on the channel asymmetry parameter A .

Definition 2 (Error class). We state that two error patterns are in the same class if they have the same amount of Pauli \mathbf{X} , \mathbf{Y} , and \mathbf{Z} errors.

In general, the error probability of an error-correcting code of length n is

$$\rho_L = \sum_{\mathbf{E} \in \mathcal{C}_n} \mathbb{P}\{\text{error}|\mathbf{E}\} \mathbb{P}\{\mathbf{E}\} \quad (7)$$

where \mathcal{C}_n is the set of all possible error classes over n qubits, $\mathbb{P}\{\text{error}|\mathbf{E}\}$ is the probability to have an error given the particular error class \mathbf{E} , and $\mathbb{P}\{\mathbf{E}\}$ is the occurrence probability

of \mathbf{E} . Since the probability $\mathbb{P}\{\text{error}|\mathbf{E}\}$ depends only on how many \mathbf{X} , \mathbf{Y} , and \mathbf{Z} the error \mathbf{E} contains, we define $f_j(i, \ell)$ as the fraction of errors of weight j with i Pauli \mathbf{Z} and ℓ Pauli \mathbf{X} errors that are not corrected. Then, we can write

$$\rho_L = \sum_{j=1}^n \binom{n}{j} (1-\rho)^{n-j} \rho^j (1-\beta_j) \quad (8)$$

where

$$1 - \beta_j = \frac{1}{\rho^j} \sum_{i=0}^j \binom{j}{i} p_Z^i \sum_{\ell=0}^{j-i} \binom{j-i}{\ell} p_X^\ell p_Y^{j-i-\ell} f_j(i, \ell). \quad (9)$$

Considering a symmetric error correcting code with bounded distance decoding which corrects up to e_g errors, we have that $f_j(i, \ell) = 0$ for $j \leq e_g$ and $f_j(i, \ell) = 1$ otherwise. In the case of an asymmetric code able to correct e_g generic errors plus e_Z Pauli \mathbf{Z} errors (see Section III-B), $f_j(i, \ell) = 0$ for $j \leq e_g$, $f_j(i, \ell) = 0$ for $e_g < j \leq e_g + e_Z$ and $i \geq e_Z$, and $f_j(i, \ell) = 1$ otherwise. For channels with $p_X = p_Y$ (e.g., depolarizing and asymmetric) we have that

$$1 - \beta_j = \frac{1}{(A+2)^j} \sum_{i=0}^j A^i \sum_{\ell=0}^{j-i} \binom{j}{i} \binom{j-i}{\ell} f_j(i, \ell). \quad (10)$$

For a symmetric code, starting from (8) we obtain the upper bound

$$\begin{aligned} \rho_L \leq & (1 - \beta_{t+1}) \binom{n}{t+1} \rho^{t+1} (1 - \rho)^{n-t-1} \\ & + \sum_{j=t+2}^n \binom{n}{j} (1 - \rho)^{n-j} \rho^j. \end{aligned} \quad (11)$$

Also, we can approximate the logical error rate for $\rho \ll 1$ as

$$\rho_L \approx (1 - \beta_{t+1}) \binom{n}{t+1} \rho^{t+1}. \quad (12)$$

Note that equation (12) differs from (2) in that the latter assumes that all errors with weight greater than t are not correctable. The asymptotic slope in log-log domain remains $t+1$, but with an offset depending on $(1 - \beta_{t+1})$, compared to (2).

In a similar way, we can find the asymptotic error correction capability of an asymmetric

code. In particular, for $\rho \ll 1$ the performance of the code becomes

$$\begin{aligned}\rho_L \approx & (1 - \beta_{e_g+e_Z+1}) \binom{n}{e_g + e_Z + 1} \rho^{e_g+e_Z+1} \\ & + (1 - \beta_{e_g+1}) \binom{n}{e_g + 1} \rho^{e_g+1}.\end{aligned}\quad (13)$$

As indicated by (8) and its approximations, to calculate the performance of quantum codes we now need to determine the fraction of correctable errors β_j .

V. WEIGHT ENUMERATORS FOR UNDETECTABLE ERRORS FROM QUANTUM MACWILLIAMS IDENTITIES

A. Undetectable Error WE

Definition 3 (Logical operators). The logical operators of a $[[n, k, d]]$ QECC are the elements of the set $\mathcal{N}(\mathcal{S}) \setminus S$, namely the operators that commute with the stabilizer but are not contained in it.

Definition 4 (Undetectable errors). The undetectable errors operators are those coincident with the logical operators. They transform a codeword into another codeword and are therefore undetectable.

Thus, the set of logical operators coincides with the set of undetectable errors. In the following, we will use the two terms interchangeably.

We then define the *undetectable errors weight enumerator* for a $[[n, k, d]]$ quantum code as

$$L(z) = \sum_{w=0}^n L_w z^w \quad (14)$$

where L_w is the number of undetectable errors (logical operators) of weight w .

The following original theorem describes how to derive the WE for the undetectable errors, starting from the generators of the code.

Theorem 1. The undetectable errors WE of an $[[n, k, d]]$ stabilizer quantum code can be computed as

$$L(z) = \frac{1}{2^k} B(z) - \frac{1}{4^k} A(z) \quad (15)$$

with $A(z) = \sum_{w=0}^n A_w z^w$ and $B(z) = \sum_{w=0}^n B_w z^w$.

The A_w can be computed as

$$A_w = 4^k \sum_{\mathbf{E}_w} |\mathbf{E}_w \cap \mathcal{S}| \quad (16)$$

where \mathbf{E}_w contains exactly w Pauli operators different from the identity, and the sum in (16) is over all \mathbf{E}_w of weight w . The B_w can be computed as

$$B_w = \frac{1}{2^n} \sum_{\ell=0}^n \sum_{s=0}^w \binom{\ell}{s} \binom{n-\ell}{w-s} (-1)^s 3^{w-s} A_\ell. \quad (17)$$

Proof: Consider an operator $\mathbf{E}_w \in \mathcal{G}_n$ containing exactly d Pauli operators different from the identity. For any two hermitian operators \mathbf{O}_1 and \mathbf{O}_2 we can introduce two WEs A_w and B_w [39], [40]

$$A_w = \sum_{\mathbf{E}_w} \text{tr}(\mathbf{E}_w \mathbf{O}_1) \text{tr}(\mathbf{E}_w \mathbf{O}_2) \quad (18)$$

$$B_w = \sum_{\mathbf{E}_w} \text{tr}(\mathbf{E}_w \mathbf{O}_1 \mathbf{E}_w \mathbf{O}_2) \quad (19)$$

where the sum is over all the \mathbf{E}_w of weight w , and $w = 0, \dots, n$. In the case in which $\mathbf{O}_1 = \mathbf{O}_2 = \Pi_{\mathcal{C}}$, the projector onto a $[[n, k, d]]$ binary stabilizer code, $A(z)$ and $B(z)$ carry some important properties of the code. Indeed, let $\mathbf{G}_i \in \mathcal{S}$, with $i = 1, \dots, n-k$, generators of the stabilizer group of a code, then [41]

$$\Pi_{\mathcal{C}} = \frac{1}{2^{n-k}} \prod_{i=1}^{n-k} (\mathbf{I} + \mathbf{G}_i) = \frac{1}{2^{n-k}} \sum_{\mathbf{S} \in \mathcal{S}} \mathbf{S}. \quad (20)$$

It can be shown [41] that the WE $A(z)$ defined in (18) is proportional to the stabilizer WE

$$\frac{1}{4^k} A(z) = \sum_{w=0}^n \sum_{\mathbf{E}_w} |\mathbf{E}_w \cap \mathcal{S}| z^w. \quad (21)$$

Moreover, $B(z)$ is proportional to the normalizer WE

$$\frac{1}{2^k} B(z) = \sum_{w=0}^n \sum_{\mathbf{E}_w} |\mathbf{E}_w \cap \mathcal{N}(\mathcal{S})| z^w. \quad (22)$$

In order to find the relation between A_w and B_w we write the associated WEs in the form

$$A(v, z) = \sum_{w=0}^n A_w v^{n-w} z^w \quad \text{and} \quad B(v, z) = \sum_{w=0}^n B_w v^{n-w} z^w. \quad (23)$$

These two polynomials are related through the quantum MacWilliam identities [40]–[42]

$$B(v, z) = A\left(\frac{v+3z}{2}, \frac{v-z}{2}\right). \quad (24)$$

Using (24) in (23) we get (17). Finally, the number of undetectable errors of weight w is given by the number of operators of weight w which commute with \mathcal{S} , given in (22), minus the number of stabilizers of weight w , given by (21), which leads to (15). ■

The evaluation of (16) can be carried out by direct inspection of \mathcal{S} for small code sizes, or more in general by using the tools for the computation of the weight distribution of classical codes as discussed in Section V-B.

For example, let's consider the $[[3,1]]$ repetition code, able to correct one bit flip error. In this case, we have $\mathbf{G}_1 = \mathbf{Z}_1\mathbf{Z}_2$, $\mathbf{G}_2 = \mathbf{Z}_2\mathbf{Z}_3$. Considering $\mathbf{O}_1 = \mathbf{O}_2 = \Pi_C$, we have from (20) that the stabilizer is $\mathcal{S} = \{\mathbf{I}_1\mathbf{I}_2\mathbf{I}_3, \mathbf{Z}_1\mathbf{Z}_2, \mathbf{Z}_2\mathbf{Z}_3, \mathbf{Z}_1\mathbf{Z}_3\}$. If we combine (20) and (18), we obtain $\frac{1}{4}A(z) = 1 + 3z^2$. Then we use (17) to compute $\frac{1}{2}B(z) = 1 + 3z + 3z^2 + 9z^3$. Finally, the undetectable errors WE is: $L(z) = 3z + 9z^3$.

In the following we will use Theorem 1 in order to compute the performance for arbitrary $[[n, k, d]]$ stabilizer codes, assuming a ML complete decoder, or a MWPM in the case of surface codes.

B. Estimation of β_j via MacWilliam Identities

Now we show that it is possible to estimate the β_j parameters with no need of simulations. In doing so, we will perform the following steps:

- Firstly, it is necessary to find the value of $A(z)$ of the $[[n, k, d]]$ code that we want to study. A trivial way to obtain this quantity is to compute all the linear combinations among the set of generators. Alternatively, it is possible to consider the connection between stabilizer codes and codes over the Galois field $GF(4)$ by identifying the operators \mathbf{I} , \mathbf{X} , \mathbf{Z} and \mathbf{Y} with the four elements of the field [15], [43]. Hence, the evaluation of $A(z)$ can be seen as the computation of the weight distribution of classical codes. Even if this turns out to be an NP-hard problem [44], many efficient algorithms for calculating the weight distribution and minimum weight have been developed [45]–[47]. Some of them are also implemented in the software tools related to coding theory, such as MAGMA [48].

- Using (17) for each value of $w = 0, \dots, n$, it is straightforward to obtain $B(z)$. Then, from (15) we derive the undetectable errors WE, $L(z)$.
- Since we are interested in the value of β_j , we have to find the total number of errors of weight $w = j$ that can cause an undetected error. We will indicate this quantity as C_j . In order to compute it, we need to consider not only $L(z)$ but also the structure of the stabilizer.
- Finally, we evaluate β_j as

$$\beta_j = 1 - \frac{C_j}{\binom{n}{j} (A+2)^j}. \quad (25)$$

In the case of a $[[n, k, d]]$ stabilizer code we can find an explicit expression for C_j

$$C_j = \sum_{i=0}^j A^i \sum_{\ell=0}^{j-i} \sum_w L_w(i, \ell) \cdot \mu_j(i, \ell) \quad (26)$$

where $L_w(i, \ell)$ stands for the number of logical operators of weight w that can be caused by the combined action of errors of weight j (composed by i \mathbf{Z} and ℓ \mathbf{X} Pauli operators) and $w - j$ correction operators, and $\mu_j(i, \ell)$ refers to the number of different patterns of errors with weight j that can realize the corresponding logical operator. Note that (25) and (10) are equivalent, since

$$\sum_w L_w(i, \ell) \cdot \mu_j(i, \ell) = \binom{n}{j} \binom{j}{i} \binom{j-i}{\ell} f_j(i, \ell). \quad (27)$$

In particular, on both sides of (27) we find the total number of errors within the error class identified by i operators of type \mathbf{Z} and ℓ operators of type \mathbf{X} . We remark that different types of logical operators of the same weight may require to be treated differently. For instance, this can happen if the code is asymmetrically degenerate with respect to the different Pauli operators, like in the Shor $[[9,1,3]]$ code. Furthermore, this feature can also depend on the decoding, as in the case of surface codes with a MWPM decoder.

In the following, we provide some examples over a depolarizing channel ($A = 1$), in order to clarify the reasoning behind the evaluation of C_j .

Firstly, consider the $[[5, 1, 3]]$ perfect code [49], with

$$\begin{aligned} \mathbf{G}_1 &= \mathbf{X}_1 \mathbf{Z}_2 \mathbf{Z}_3 \mathbf{X}_4 & \mathbf{G}_2 &= \mathbf{X}_2 \mathbf{Z}_3 \mathbf{Z}_4 \mathbf{X}_5 \\ \mathbf{G}_3 &= \mathbf{X}_1 \mathbf{X}_3 \mathbf{Z}_4 \mathbf{Z}_5 & \mathbf{G}_4 &= \mathbf{Z}_1 \mathbf{X}_2 \mathbf{X}_4 \mathbf{Z}_5 \end{aligned}$$

Using Theorem 1 we first obtain $L(z) = 30z^3 + 18z^5$. Then, we have

$$\beta_2 = 1 - \frac{30 \cdot 3}{\binom{5}{2} 3^2} = 0 \quad (28)$$

where we have evaluated C_j considering that three different combinations of errors of weight $w = 2$ can produce a logical operator of $w = 3$. This result was expected since the code is perfect.

A more interesting case is that of the $[[7, 1, 3]]$ Steane code [50]. Its generators are

$$\begin{aligned} \mathbf{G}_1 &= \mathbf{X}_1 \mathbf{X}_3 \mathbf{X}_5 \mathbf{X}_7 & \mathbf{G}_2 &= \mathbf{X}_2 \mathbf{X}_3 \mathbf{X}_6 \mathbf{X}_7 & \mathbf{G}_3 &= \mathbf{X}_4 \mathbf{X}_5 \mathbf{X}_6 \mathbf{X}_7 \\ \mathbf{G}_4 &= \mathbf{Z}_1 \mathbf{Z}_3 \mathbf{Z}_5 \mathbf{Z}_7 & \mathbf{G}_5 &= \mathbf{Z}_2 \mathbf{Z}_3 \mathbf{Z}_6 \mathbf{Z}_7 & \mathbf{G}_6 &= \mathbf{Z}_4 \mathbf{Z}_5 \mathbf{Z}_6 \mathbf{Z}_7. \end{aligned}$$

Using Theorem 1 we compute the WE as $L(z) = 21z^3 + 126z^5 + 45z^7$. Then, assuming a ML decoder, we calculate

$$\beta_2 = 1 - \frac{21 \cdot 3 + \binom{2}{3} \cdot 21 \cdot 3 \cdot 2}{\binom{7}{2} 3^2} = \frac{2}{9} \simeq 0.22. \quad (29)$$

To derive this value we observed that, unlike the perfect code, each logical operator of $w = 3$ is composed of only one kind of Pauli operator. Moreover, we have to consider that each one of these \mathbf{X} (\mathbf{Z}) logical operators can be generated by couples of \mathbf{Z} (\mathbf{X}) errors, and also by \mathbf{XY} (\mathbf{ZY}), since errors of $w = 1$ can always be corrected. In this case, we have to take into account the position in which each error may occur, resulting in an additional multiplication by two. From (12) and (29) we obtain for the $[[7, 1, 3]]$ code

$$\rho_L \approx 16.38\rho^2 \quad , \quad \rho \ll 1. \quad (30)$$

A different example is the one regarding the $[[9, 1, 3]]$ Shor code [7], having generators

$$\begin{aligned} \mathbf{G}_1 &= \mathbf{Z}_1 \mathbf{Z}_2 & \mathbf{G}_2 &= \mathbf{Z}_2 \mathbf{Z}_3 \\ \mathbf{G}_3 &= \mathbf{Z}_4 \mathbf{Z}_5 & \mathbf{G}_4 &= \mathbf{Z}_5 \mathbf{Z}_6 \\ \mathbf{G}_5 &= \mathbf{Z}_7 \mathbf{Z}_8 & \mathbf{G}_6 &= \mathbf{Z}_8 \mathbf{Z}_9 \\ \mathbf{G}_7 &= \mathbf{X}_1 \mathbf{X}_2 \mathbf{X}_3 \mathbf{X}_4 \mathbf{X}_5 \mathbf{X}_6 & \mathbf{G}_8 &= \mathbf{X}_4 \mathbf{X}_5 \mathbf{X}_6 \mathbf{X}_7 \mathbf{X}_8 \mathbf{X}_9. \end{aligned}$$

This a distance three degenerate code. From (15) the WE results $L(z) = 39z^3 + 208z^5 + 332z^7 + 189z^9$. Assuming a ML decoder, channel errors of weight two cause the 39 unde-

tectable errors of weight three. More precisely, we obtain

$$\beta_2 = 1 - \frac{3 \cdot 3 + 27 + 27 \cdot 2 + 9 \cdot 3 + 27}{\binom{9}{2} 3^2} = \frac{5}{9} \simeq 0.56 \quad (31)$$

where the numerator is composed by the sum of \mathbf{XXX} , \mathbf{ZZZ} , \mathbf{ZZY} , \mathbf{YYX} and \mathbf{YYZ} operators. Note that the actual logical operators are \mathbf{XXX} , \mathbf{ZZZ} and \mathbf{YYX} . In other cases, some Pauli operators anti-commute with at least one stabilizer, but they can be corrected. Since this code is degenerate with respect to \mathbf{Z} Pauli errors, it is necessary to treat differently the logical operators of each type. In particular, we do not multiply \mathbf{Z} operators by three since the same two \mathbf{Z} errors can cause three different \mathbf{ZZZ} logical operators. From (12) and (31) we obtain for the $[[9, 1, 3]]$ code

$$\rho_L \approx 16.2\rho^2 \quad , \quad \rho \ll 1. \quad (32)$$

Using similar reasoning, it is possible to obtain the β_j values for the surface code with MWPM decoding. Considering the $[[13, 1, 3]]$ surface code, from (15) we first find $L(z) = 6z^3 + 24z^4 + 75z^5 + 240z^6 + 648z^7 + 1440z^8 + 2538z^9 + 3216z^{10} + 2634z^{11} + 1224z^{12} + 243z^{13}$. Note that in this case, we have also logical operators of weight four. While in the three cases above we computed β_2 for a ML decoder, for surface codes we consider what happens with the MWPM decoder. To this aim, we need to analyze how channel errors of weight $j = 2$ cause logical operators. Moreover, we need to distinguish different logical operators of the same weight, due to the MWPM decoding. For example, $L_4 = 24$ has to be divided into two terms: 16+8. Indeed, among the 24 logical operators of weight $w = 4$, only 16 are composed by \mathbf{XXXX} and \mathbf{ZZZZ} Pauli operators. The remaining eight are of type \mathbf{YYXZ} as in Fig. 2 (e), (f). Note that, since generators are composed of only \mathbf{X} or only \mathbf{Z} operators, channel errors can never cause a \mathbf{Y} correction operator. As a consequence, one of these eight logical operators can be caused only by \mathbf{YY} errors in the same positions as those in the logical operator. Considering all cases we obtain

$$\beta_2 = 1 - \frac{6 \cdot 3 \cdot 4 + 16 \cdot \frac{3}{2} \cdot 4}{\binom{13}{2} 3^2} = \frac{89}{117} \simeq 0.76. \quad (33)$$

In this expression we take into account the eight \mathbf{YYXZ} operators implicitly as if they had $w = 3$, since each combination of two \mathbf{Y} errors can cause a logical operator with three \mathbf{Z} or three \mathbf{X} . More precisely, for the term $16 \cdot 3/2 \cdot 4$, the factor $3/2$ is due to the presence of four different combinations of two errors that can produce a logical operator of weight $w = 4$.

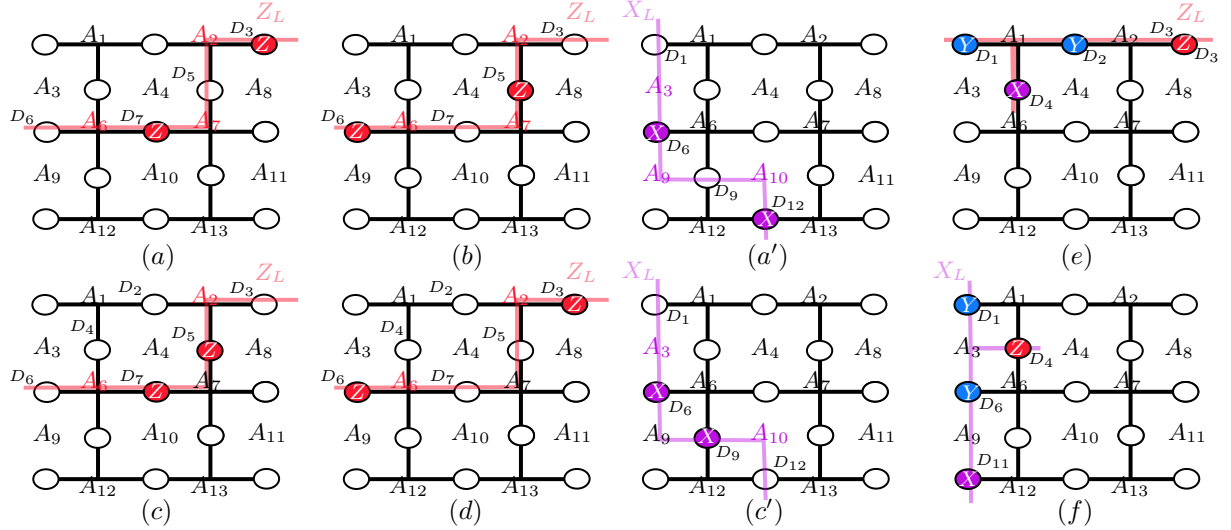


Fig. 2. Example of a logical operator of $w = 4$ for the $[[13, 1, 3]]$ surface code. \mathbf{Z} , \mathbf{X} , and \mathbf{Y} errors on qubits are depicted in red, purple, and blue, respectively. (a) \mathbf{Z}_L occurs if \mathbf{Z} correction operators are applied on data qubits D_5 and D_6 . The errors are corrected if the MWPM decoder applies \mathbf{Z} on D_3 and D_7 . (b) \mathbf{Z}_L occurs if \mathbf{Z} correction operators are applied on D_3 and D_7 . The errors are corrected if the MWPM decoder applies \mathbf{Z} on D_5 and D_6 . (c) \mathbf{Z}_L occurs if \mathbf{Z} correction operators are applied on D_3 and D_6 . The MWPM decoder could apply also \mathbf{Z} operators on D_5 and D_7 , correcting the error, or on D_2 and D_4 , causing a different logical operator. (d) \mathbf{Z}_L occurs if \mathbf{Z} correction operators are applied on D_5 and D_7 . The MWPM decoder could apply also \mathbf{Z} operators on D_3 and D_6 or on D_2 and D_4 . (a', c') Analogous examples for \mathbf{X}_L logical operator. (e, f) Logical operators of $w = 4$ with \mathbf{Y}_L errors.

Two combinations are always corrected, while the others cause a logical operator. However, half of them must be taken into account only once, because they are common to two different logical operators, producing the factor $3/2$. An example is shown in Fig. 2. In addition, factor 4 stands for the possible error classes $\mathbf{XX}(\mathbf{ZZ})$, $\mathbf{XY}(\mathbf{ZY})$ and $\mathbf{YX}(\mathbf{YZ})$, since we are sure that errors of $w = 1$ are always corrected, and \mathbf{YY} . From (12) and (33) we obtain for the $[[13, 1, 3]]$ surface code over the depolarizing channel

$$\rho_L \approx 18.74\rho^2 \quad , \quad \rho \ll 1. \quad (34)$$

Using (26) it is also possible to obtain the value of β_j for asymmetric channels. For instance, in the case of the $[[13, 1, 3]]$ surface code over a phase flip channel, we have only three \mathbf{Z} logical operators with $w = 3$ and eight \mathbf{Z} logical operators with $w = 4$, giving

$$\beta_2 = 1 - \frac{3 \cdot 3 + 8 \cdot \frac{3}{2}}{\binom{13}{2}} = \frac{19}{26} \simeq 0.73. \quad (35)$$

C. β_j by exhaustive search

A different approach to compute the β_j coefficients for a given code and a given decoder is by exhaustive search. In Tab. I we report for some surface codes the percentage of non-

TABLE I
FRACTION OF NON-CORRECTABLE ERROR PATTERNS PER ERROR CLASS OF SURFACE CODES USING MINIMUM WEIGHT PERFECT MATCHING.

Code	XX	XZ	XY	ZZ	ZY	YY				
Code	XXX	XXZ	XXY	XZZ	XZY	XYY	ZZZ	ZZY	ZYY	YYY
$[[13, 1, 3]]$	0.27	0	0.27	0.27	0.27	0.51				
$[[23, 1, 3/5]]$	0.16	0	0.16	0	0	0.15				
							$1 - \beta_2(A)$			$1 - \beta_3(A)$
Code	$A = 1$	$A = 10$	$A = 100$	$A \rightarrow \infty$			$A = 1$	$A = 10$	$A = 100$	$A \rightarrow \infty$
$[[13, 1, 3]]$	0.24	0.233	0.265	0.27			0.52	0.48	0.523	0.53
$[[23, 1, 3/5]]$	0.07	0.0044	$6 \cdot 10^{-5}$	0			0.203	0.0736	0.0778	0.08
$[[41, 1, 5]]$	0	0	0	0			0.014	0.019	0.023	0.024

correctable errors for each error class $f_j(i, \ell)$, which we have evaluated by exhaustive search with a MWPM decoder. In doing so we exploited the Lemon C++ library [51], which provides an efficient implementation of graphs and networks algorithms. For example, in the case of the $[[13, 1, 3]]$ surface code, it results $f_2(0, 2) = 0.27$. Once we have $f_j(i, \ell)$, we can compute the value of $1 - \beta_j$ for $A = 1$, $A = 10$, $A = 100$, and $A \rightarrow \infty$, by weighting the percentages of non-correctable errors as indicated by (10). Note that the value of $1 - \beta_j$ for $A \rightarrow \infty$ is equivalent to $f_j(i, \ell)$ of the class with j Pauli Z . From Tab. I, we observe that, as anticipated, surface codes can correct a large number of errors above the guaranteed error correction capability. For example, the $[[13, 1, 3]]$ can correct about 75% and 50% of the error patterns of weight 2 and 3, respectively.

Increasing the distance of the code, the exhaustive search for deriving the β_j could become infeasible. However, as can be observed in Tab. I, the value of β_j for $A \rightarrow \infty$ is close to that for $A = 1$. Hence, it is possible to obtain a good estimation of β_j over a depolarizing channel taking into account just Z errors, which require considering only $\binom{n}{j}$ patterns.

VI. NUMERICAL RESULTS

In this section, we evaluate the performance of some codes, in terms of logical error rate ρ_L vs. physical error rate ρ , based on the analysis described previously. Also, to highlight

the potential advantage of QECC, we define the code-effective threshold ρ_{thr} as

$$\rho_{\text{thr}} = \max \left\{ \rho : \rho_L \leq 10^{-\gamma} \rho \right\}. \quad (36)$$

This threshold is the value of ρ such that a QECC gives a performance boost in terms of logical error rate of 10^γ , with $\gamma \geq 0$, compared to the uncoded case. In [38], the authors define a pseudo-threshold which is equivalent to the code-effective threshold when $\gamma = 0$. Despite the fact that quantum codes could improve the performance for some values of ρ , if the performance boost is small, implementing them may not be worth it. For this reason, we generalize this definition to target a performance boost requirement. One method to compute this threshold could be to proceed by Monte Carlo simulations to find the intersection with the shifted uncoded performance $\rho_L = 10^{-\gamma} \rho$. However, using (8) or its asymptotic approximations it is possible to derive this value analytically. For example, for a symmetric code, we use (12) to approximate the code-effective threshold as

$$\tilde{\rho}_{\text{thr}} = \sqrt[t]{\frac{1}{10^\gamma (1 - \beta_{t+1}) \binom{n}{t+1}}}. \quad (37)$$

In the following figures, we will show $\tilde{\rho}_{\text{thr}}$ to delimit the values of ρ where the QECC gives an advantage of γ orders of magnitude with respect to the uncoded case.

1) *Comparison between analysis and simulation for the [[9, 1, 3]] code.* To verify the correctness of the proposed analytical approach we start by studying the Shor code. Fig. 3 shows, for the [[9,1,3]] code, a comparison between the upper bound (11), the asymptotic approximation (12) (which, since here $\beta_2 = 0.56$, becomes (32)), and the logical error rate obtained via Monte Carlo simulations, adopting an ML decoder. It can be seen that the results are in perfect agreement for $\rho < 0.1$, while there is a small gap for larger ρ . This gap arises because (11) implicitly assumes $\beta_j = 0$ for $j \geq 3$, while the Shor code is able to correct also a little percentage of errors of weight $j \geq 3$, as for instance \mathbf{X} errors in three different qubit triplets ($\mathbf{X}_1 \mathbf{X}_4 \mathbf{X}_7$). Moreover, in the plot, we report the error probability with the BD decoder, computed using (1), which has the same trend as the ML decoder. The gap between the two curves is due to the fraction of weight two errors which are corrected by the ML decoder.

2) *Exact analysis.* In Fig. 4 we verify the performance as given by equation (8) over depolarizing and phase flip channels, taking into account many values of β_j . To this aim, we compare the analytical formulas with simulations for the [[13, 1, 3]] surface code over a

depolarizing channel, and for the $[[23, 1, 3/5]]$ surface code over a phase flip channel. For both codes, we consider the MWPM decoder. Specifically, for the $[[13, 1, 3]]$ surface code over depolarizing channel, we plot (8) using $(\beta_2, \beta_3, \beta_4, \beta_5, \beta_6) = (0.76, 0.48, 0.48, 0.46, 0.5)$ where (β_2, β_3) are computed by exhaustive search according to (10), while $(\beta_4, \beta_5, \beta_6)$ are approximated using the values computed for $A \rightarrow \infty$. The β_j with $j > 6$ are set to zero. Similarly, for the $[[23, 1, 3/5]]$ surface code over a phase flip channel, we used $(\beta_3, \beta_4, \beta_5, \beta_6, \beta_7) = (0.92, 0.76, 0.59, 0.52, 0.49)$, and $\beta_j = 0$ for $j > 7$. In the figure, we also plot their asymptotic approximations (12), with $\beta_2 = 0.76$ and $\beta_3 = 0.92$ for the $[[13, 1, 3]]$ and the $[[23, 1, 3/5]]$ codes, respectively. As expected, the approximations are tight for $\rho \ll 1$, allowing to estimate logical error rates not achievable by Monte Carlo simulations.

3) *Analysis of several quantum codes.* In Fig. 5 we show the asymptotic approximation of the logical error rate for the $[[5, 1, 3]]$ perfect code, the $[[7, 1, 3]]$ Steane code, the $[[9, 1, 3]]$ Shor code, the $[[13, 1, 3]]$ surface code, and the $[[41, 1, 5]]$ surface code. In doing so, we use (12) and the values of β_2 obtained in Section V-B. In particular, we can see that the $[[5, 1, 3]]$ perfect code has the best error correction capability among the codes with distance $d = 3$, despite it is not able to correct any error of weight $j \geq 2$. This is because it is shorter than the others, so less prone to channel errors. For the same reason, Steane and Shor codes show almost the same performance even if the former has a much smaller value of β_2 . Finally, surface codes pay the price of all the implementation benefits that their lattice provides. For instance, even if the $[[13, 1, 3]]$ surface code is able to correct many errors of weight $j = 2$, it requires a large number of redundancy qubits. The same conclusion can be drawn by comparing the code-effective thresholds. For instance, for a boost of one order of magnitude, $\gamma = 1$, we obtain $\tilde{\rho}_{\text{thr}} = 0.01, 0.0061, 0.0062, 0.0053, 0.0261$, for $n = 5, 7, 9, 13$ and 41, respectively.

4) *Code effective threshold.* In Tab. II we report the code effective threshold, obtained with (37), for the $[[13, 1, 3]]$ and the $[[41, 1, 5]]$ surface codes over the depolarizing channel, and for the $[[23, 1, 3/5]]$ asymmetric surface code on a phase flip channel. We note that the threshold increases from $\tilde{\rho}_{\text{thr}} = 0.0534$ to $\tilde{\rho}_{\text{thr}} = 0.0824$ when we pass from the $[[13, 1, 3]]$ to the $[[41, 1, 5]]$ surface code. As expected, the threshold value increases with the error correction capability of the code. For the $[[23, 1, 3/5]]$ asymmetric surface code on a phase flip channel, we obtain the asymptotic performance by using $t = e_g + e_z = 2$ in (37). The resulting threshold, $\tilde{\rho}_{\text{thr}} = 0.086$, is higher than the previous ones. This is due to the fact that this code has distance $d_z = 5$, thus on a phase flip channel it works better than the $[[13, 1, 3]]$

TABLE II
CODE-EFFECTIVE THRESHOLDS FOR SOME SURFACE CODES.

	[[13, 1, 3]]	[[23, 1, 3/5]]	[[41, 1, 5]]
$\gamma = 0$	0.0534	0.0861	0.0824
$\gamma = 1$	0.00534	0.0272	0.0261

code (which has a smaller distance), and also of the [[41, 1, 5]] code (which uses a larger number of qubits).

5) *Codes over asymmetric channels.* In Fig. 6, we study the performance over an asymmetric channel with asymmetry parameter $A = 10$. Specifically, we have determined the asymptotic approximations using (4) and β_j as from Tab. I, which accounts for the error rate of codes over channels with different error probabilities related to different kinds of errors (Z , X and Y). It is interesting to note that, for all kinds of bias of the channel ($A = 1, 10, 100$), the simulated logical error rate has the same behavior of the bound error probability, but with a gap between each couple of curves. This gap is due to the capability of surface codes to correct many errors of weight $w \geq t+1$. However, since not all the errors of weight $w = t+1$ can be corrected, we have $\beta_{t+1} > 0$, and this makes the asymptotic slope to be $t+1$, no matter how small is β_{t+1} . Moreover, we computed the asymptotic approximations of the logical error rate for the [[23, 1, 3/5]] surface code, over the same symmetric and asymmetric channels using (13). The values of β_j used in this simulation are shown in Tab. I. We can observe that, for $\rho \ll 1$, these curves are tight to the respective Monte Carlo simulations.

VII. CONCLUSIONS

We have derived the weight enumerator for the undetectable errors of stabilizer codes starting from the quantum MacWilliams identities. We have then shown how it is possible to analytically evaluate the logical error probability of a generic stabilizer code. We applied the proposed approach to the analytical performance evaluation of Steane and Shor codes assuming ML decoding, and of surface codes with MWPM decoding, providing analytical expressions and comparison with simulations, over symmetric and asymmetric quantum channels. For example, we express the asymptotic error rate in the form $\eta\rho^{t+1}$ where η , which depends on the fraction of channel errors of weight $t+1$ that the decoder is able to correct, is calculated with the proposed method. In particular, for a surface code with minimum distance d , the possibility to use decoders like the MWPM, which allows correction

of many patterns with more than $\lfloor (d - 1)/2 \rfloor$ qubit errors, gives a considerable advantage with respect to bounded distance decoders.

REFERENCES

- [1] H. J. Kimble, “The quantum internet,” *Nature*, vol. 453, no. 7198, p. 1023, 2008.
- [2] J. Preskill, “Quantum Computing in the NISQ era and beyond,” *Quantum*, vol. 2, p. 79, Aug. 2018.
- [3] *Quantum Networks for Open Science Workshop*. Rockville, MD, USA: Office of Science US Department of Energy, 2018.
- [4] E. Grumblig and M. Horowitz, Eds., *Quantum Computing: Progress and Prospects*. Washington, DC: The National Academies Press, 2019.
- [5] S. Wehner, D. Elkouss, and R. Hanson, “Quantum internet: A vision for the road ahead,” *Science*, vol. 362, no. 6412, 2018.
- [6] A. S. Cacciapuoti, M. Caleffi, R. Van Meter, and L. Hanzo, “When entanglement meets classical communications: Quantum teleportation for the quantum Internet,” *IEEE Transactions on Communications*, vol. 68, no. 6, pp. 3808–3833, 2020.
- [7] P. W. Shor, “Scheme for reducing decoherence in quantum computer memory,” *Phys. Rev. A*, vol. 52, pp. R2493–R2496, Oct 1995.
- [8] R. Laflamme, C. Miquel, J. P. Paz, and W. H. Zurek, “Perfect quantum error correcting code,” *Physical Review Letters*, vol. 77, no. 1, p. 198, 1996.
- [9] D. Gottesman, “Class of quantum error-correcting codes saturating the quantum Hamming bound,” *Phys. Rev. A*, vol. 54:1862, 1996.
- [10] E. Knill and R. Laflamme, “Theory of quantum error-correcting codes,” *Phys. Rev. A*, vol. 55, pp. 900–911, Feb 1997.
- [11] A. S. Fletcher, P. W. Shor, and M. Z. Win, “Structured near-optimal channel-adapted quantum error correction,” *Phys. Rev. A*, vol. 77, p. 012320, Jan 2008.
- [12] M. A. Nielsen and I. L. Chuang, *Quantum Computation and Quantum Information: 10th Anniversary Edition*. Cambridge University Press, 2010.
- [13] J. ur Rehman and H. Shin, “Entanglement-free parameter estimation of generalized Pauli channels,” *Quantum*, vol. 5, p. 490, 2021.
- [14] A. M. Steane, “Error correcting codes in quantum theory,” *Phys. Rev. Lett.*, vol. 77, no. 5, pp. 793–797, 1996.
- [15] D. Gottesman, “An introduction to quantum error correction and fault-tolerant quantum computation,” *arXiv preprint quant-ph/0904.2557*, 2009.
- [16] B. M. Terhal, “Quantum error correction for quantum memories,” *Rev. Mod. Phys.*, vol. 87, pp. 307–346, Apr 2015.
- [17] S. Muralidharan, L. Li, J. Kim, N. Lütkenhaus, M. D. Lukin, and L. Jiang, “Optimal architectures for long distance quantum communication,” *Scientific reports*, vol. 6, p. 20463, 2016.
- [18] J. Roffe, “Quantum error correction: an introductory guide,” *Contemporary Physics*, vol. 60, no. 3, pp. 226–245, jul 2019.
- [19] Z. Babar, D. Chandra, H. V. Nguyen, P. Botsinis, D. Alanis, S. X. Ng, and L. Hanzo, “Duality of quantum and classical error correction codes: Design principles and examples,” *IEEE Communications Surveys Tutorials*, vol. 21, no. 1, pp. 970–1010, Firstquarter 2019.
- [20] M. Chiani, A. Conti, and M. Z. Win, “Piggybacking on quantum streams,” *Physical Review A*, vol. 102, no. 1, jul 2020.

- [21] F. Zoratti, G. De Palma, and V. Giovannetti, “Improving the speed of variational quantum algorithms for quantum error correction,” *arXiv preprint arXiv:2301.05273*, 2023.
- [22] D. Ostrev, D. Orsucci, F. Lázaro, and B. Matuz, “Classical product code constructions for quantum Calderbank-Shor-Steane codes,” 2022. [Online]. Available: <https://arxiv.org/abs/2209.13474>
- [23] L. Ioffe and M. Mézard, “Asymmetric quantum error-correcting codes,” *Physical Review A*, vol. 75, no. 3, p. 032345, 2007.
- [24] P. K. Sarvepalli, A. Klappenecker, and M. Rötteler, “Asymmetric quantum codes: constructions, bounds and performance,” *Proceedings of the Royal Society A: Mathematical, Physical and Engineering Sciences*, vol. 465, no. 2105, pp. 1645–1672, 2009.
- [25] D. Layden, M. Chen, P. Cappellaro *et al.*, “Efficient quantum error correction of dephasing induced by a common fluctuator,” *Physical review letters*, vol. 124, no. 2, p. 020504, 2020.
- [26] M. Chiani and L. Valentini, “Short codes for quantum channels with one prevalent Pauli error type,” *IEEE J. on Selected Areas in Information Theory*, vol. 1, no. 2, pp. 480–486, 2020.
- [27] S. B. Bravyi and A. Y. Kitaev, “Quantum codes on a lattice with boundary,” 1998.
- [28] A. G. Fowler, M. Mariantoni, J. M. Martinis, and A. N. Cleland, “Surface codes: Towards practical large-scale quantum computation,” *Physical Review A*, vol. 86, no. 3, sep 2012.
- [29] R. Acharya, I. Aleiner, R. Allen, T. I. Andersen, M. Ansmann, F. Arute, K. Arya, A. Asfaw, J. Atalaya, R. Babbush *et al.*, “Suppressing quantum errors by scaling a surface code logical qubit,” *arXiv preprint arXiv:2207.06431*, 2022.
- [30] S. Krinner, N. Lacroix, A. Remm, A. Di Paolo, E. Genois, C. Leroux, C. Hellings, S. Lazar, F. Swiadek, J. Herrmann *et al.*, “Realizing repeated quantum error correction in a distance-three surface code,” *Nature*, vol. 605, no. 7911, pp. 669–674, 2022.
- [31] Y. Zhao, Y. Ye, H.-L. Huang, Y. Zhang, D. Wu, H. Guan, Q. Zhu, Z. Wei, T. He, S. Cao, F. Chen, T.-H. Chung, H. Deng, D. Fan, M. Gong, C. Guo, S. Guo, L. Han, N. Li, S. Li, Y. Li, F. Liang, J. Lin, H. Qian, H. Rong, H. Su, L. Sun, S. Wang, Y. Wu, Y. Xu, C. Ying, J. Yu, C. Zha, K. Zhang, Y.-H. Huo, C.-Y. Lu, C.-Z. Peng, X. Zhu, and J.-W. Pan, “Realization of an error-correcting surface code with superconducting qubits,” *Phys. Rev. Lett.*, vol. 129, p. 030501, Jul 2022.
- [32] J. Preskill, “Reliable quantum computers,” *Proceedings of the Royal Society of London. Series A: Mathematical, Physical and Engineering Sciences*, vol. 454, no. 1969, pp. 385–410, 1998.
- [33] S. Bravyi, M. Suchara, and A. Vargo, “Efficient algorithms for maximum likelihood decoding in the surface code,” *Physical Review A*, vol. 90, no. 3, p. 032326, 2014.
- [34] J. P. B. Ataides, D. K. Tuckett, S. D. Bartlett, S. T. Flammia, and B. J. Brown, “The XZZX surface code,” *Nature Communications*, vol. 12, no. 1, apr 2021.
- [35] C. Horsman, A. G. Fowler, S. Devitt, and R. V. Meter, “Surface code quantum computing by lattice surgery,” *New Journal of Physics*, vol. 14, no. 12, p. 123011, dec 2012.
- [36] E. Dennis, A. Kitaev, A. Landahl, and J. Preskill, “Topological quantum memory,” *Journal of Mathematical Physics*, vol. 43, no. 9, pp. 4452–4505, sep 2002.
- [37] O. Higgott, “Pymatching: A Python package for decoding quantum codes with minimum-weight perfect matching,” *ACM Transactions on Quantum Computing*, vol. 3, no. 3, pp. 1–16, 2022.
- [38] U. Azad, A. Lipiń ska, S. Mahato, R. Sachdeva, D. Bhoumik, and R. Majumdar, “Surface code design for asymmetric error channels,” *IET Quantum Communication*, may 2022.
- [39] P. Shor and R. Laflamme, “Quantum analog of the macwilliams identities for classical coding theory,” *Physical review letters*, vol. 78, no. 8, p. 1600, 1997.

- [40] E. M. Rains, “Quantum weight enumerators,” *IEEE Transactions on Information Theory*, vol. 44, no. 4, pp. 1388–1394, 1998.
- [41] C. Cao and B. Lackey, “Quantum weight enumerators and tensor networks,” *arXiv preprint arXiv:2211.02756*, 2022.
- [42] F. MacWilliams and N. Sloane, *The theory of error-correcting codes*. Amsterdam, the Netherlands: North Holland Mathematical Library, 1977, vol. 16.
- [43] A. R. Calderbank, E. M. Rains, P. W. Shor, and N. J. A. Sloane, “Quantum error correction via codes over GF(4),” *IEEE Trans. Inf. Theory*, vol. 44, no. 4, pp. 1369–1387, 1998.
- [44] E. Berlekamp, R. McEliece, and H. Van Tilborg, “On the inherent intractability of certain coding problems (corresp.),” *IEEE Transactions on Information Theory*, vol. 24, no. 3, pp. 384–386, 1978.
- [45] T. A. Gulliver, V. K. Bhargava, and J. M. Stein, “Q-ary gray codes and weight distributions,” *Applied mathematics and computation*, vol. 103, no. 1, pp. 97–109, 1999.
- [46] I. Bouyukliev, S. Bouyuklieva, T. Maruta, and P. Piperkov, “Characteristic vector and weight distribution of a linear code,” *Cryptography and Communications*, vol. 13, no. 2, pp. 263–282, 2021.
- [47] K. Zimmermann, *Integral Hecke Modules, Integral Generalized Reed-Muller Codes, and Linear Codes*, ser. Berichte des Forschungsschwerpunktes Informations- und Kommunikationstechnik. Techn. Univ. Hamburg-Harburg, 1996. [Online]. Available: https://books.google.es/books?id=_2FamwEACAAJ
- [48] W. Bosma, J. Cannon, and C. Playoust, “The magma algebra system I: The user language,” *Journal of Symbolic Computation*, vol. 24, no. 3-4, pp. 235–265, 1997.
- [49] R. Laflamme, C. Miquel, J. P. Paz, and W. H. Zurek, “Perfect quantum error correcting code,” *Physical Review Letters*, vol. 77, no. 1, p. 198, 1996.
- [50] A. M. Steane, “Error correcting codes in quantum theory,” *Physical Review Letters*, vol. 77, no. 5, p. 793, 1996.
- [51] B. Dezső, A. Jüttner, and P. Kovács, “Lemon—an open source C++ graph template library,” *Electronic notes in theoretical computer science*, vol. 264, no. 5, pp. 23–45, 2011.

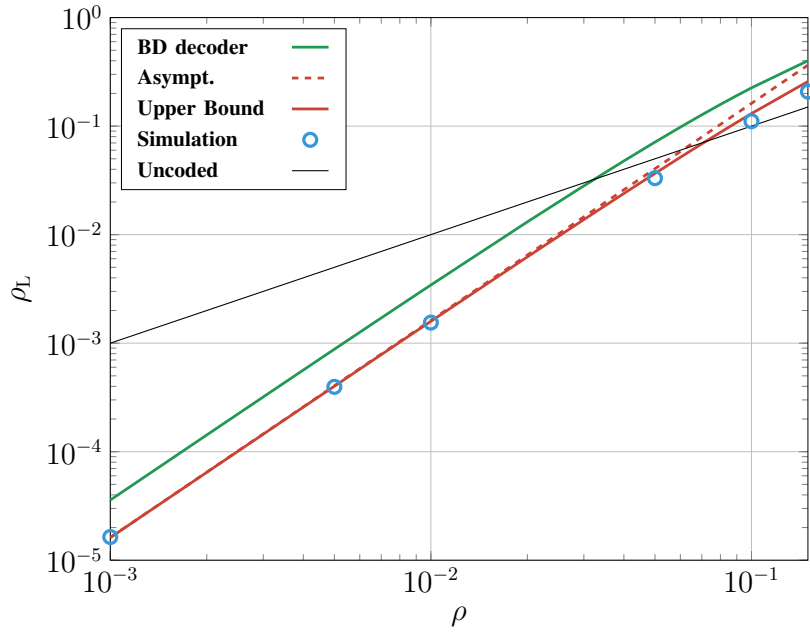


Fig. 3. Logical error rate, $[[9, 1, 3]]$ Shor code over a depolarizing channel. Comparison between theoretical analysis (curves) and simulation (symbols). The curves refer to the ML decoding upper bound (11) and the asymptotic approximation (12) with $\beta_2 = 0.56$, and the BD decoding performance (1).

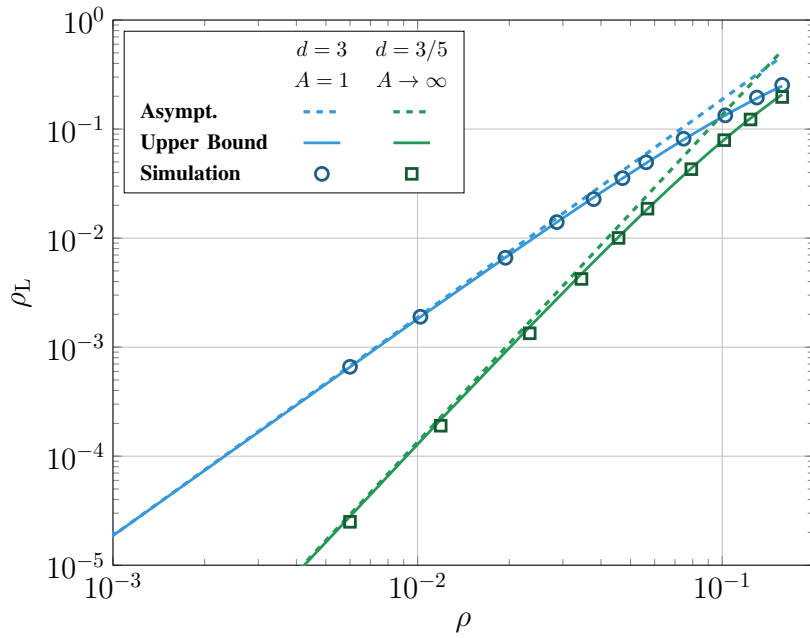


Fig. 4. Logical error rate, $[[13, 1, 3]]$ surface code over a depolarizing channel, $[[23, 1, 3/5]]$ surface code over a phase flip channel. Comparison between theoretical analysis and simulation. MWPM decoder.

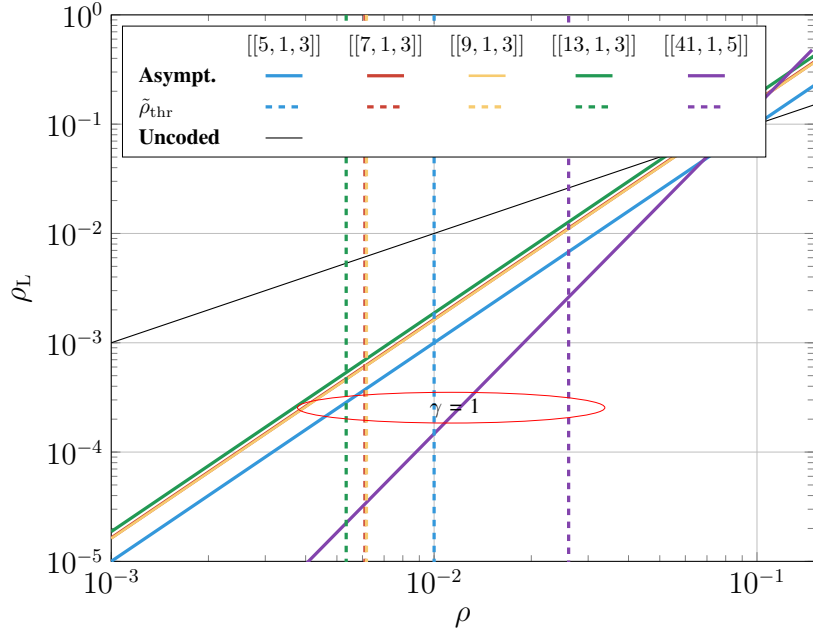


Fig. 5. Logical error rate vs. physical error rate, $[[5, 1, 3]]$ code, $[[7, 1, 3]]$ Steane code, $[[9, 1, 3]]$ Shor code, the $[[13, 1, 3]]$ surface code, and the $[[41, 1, 5]]$ surface code, over a depolarizing channel. The code-effective threshold is calculated for $\gamma = 1$.

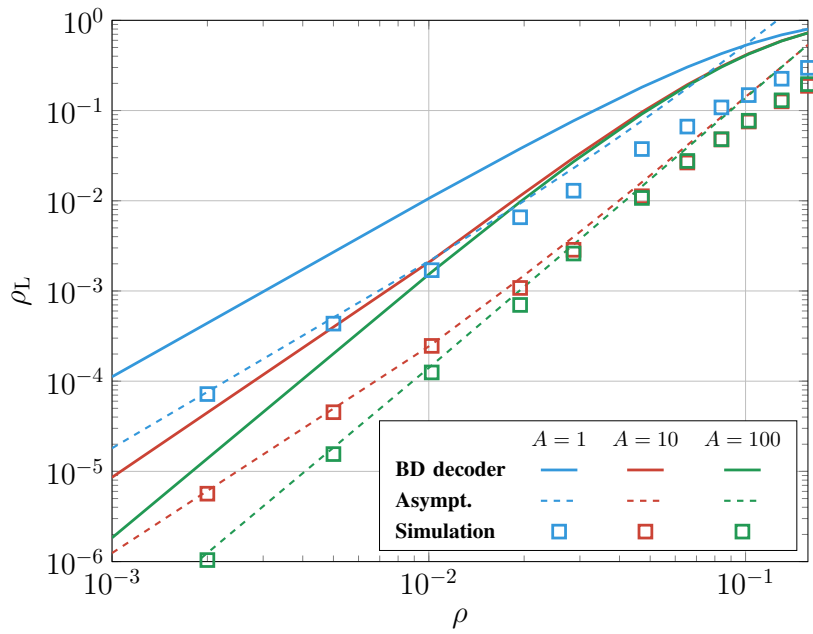


Fig. 6. Logical error rate, $[[23, 1, 3/5]]$ surface code over symmetric and asymmetric channels. Comparison between the bound (4), the asymptotic approximation (13), and the simulations with a MWPM decoder.